

Pancreatic imaging in MEN1 – comparison of conventional and somatostatin receptor positron emission tomography/computed tomography imaging in real-life setting

Iiro Kostiainen,^{1,*}  Susanna Majala,^{2,3} Jukka Schildt,⁴ Helka Parviainen,^{5,6} Salla Kauhanen,^{2,3} Hanna Seppänen,⁷ Päivi J. Miettinen,⁸ Niina Matikainen,¹ Eeva M. Ryhänen,¹ and Camilla Schalin-Jääntti¹

¹Endocrinology, Abdominal Center, Helsinki University Hospital and University of Helsinki, 00029 Helsinki, Finland

²Department of Surgery, Division of Digestive Surgery and Urology, Turku University Hospital and University of Turku, 20251 Turku, Finland

³Turku PET Centre, Turku University Hospital, 20521 Turku, Finland

⁴HUS Medical Imaging Center, Department of Clinical Physiology and Nuclear Medicine, Helsinki University Hospital and University of Helsinki, 00029 Helsinki, Finland

⁵HUS Medical Imaging Center, Department of Radiology, Helsinki University Hospital and University of Helsinki, 00029 Helsinki, Finland

⁶Department of Radiology, Vaasa Central Hospital, Wellbeing Services County of Ostrobothnia, 65130 Vaasa, Finland

⁷Department of Gastrointestinal Surgery, Translational Cancer Medicine Program, iCAN Digital Precision Cancer Medicine Flagship, Faculty of Medicine, Helsinki University Hospital and University of Helsinki, 00029 Helsinki, Finland

⁸Pediatric Research Center, New Children's Hospital, Helsinki University Hospital and University of Helsinki, 00029 Helsinki, Finland

*Corresponding author: Division of Endocrinology, Department of Medicine, Helsinki University Central Hospital, P.O. Box 340, FI-00029, Helsinki, Finland.
Email: iiro.kostiainen@hus.fi

Abstract

Objective: Pancreatic neuroendocrine tumors (panNETs) are the leading cause of death in patients with multiple endocrine neoplasia type 1 (MEN1). The role of somatostatin receptor positron emission tomography/computed tomography (SSTR PET/CT) in MEN1 has not been established. The aim was to assess pancreatic imaging in MEN1 in a real-life setting.

Design: Fifty-eight patients with MEN1 [median age 40 (range 16–72) years] underwent SSTR PET/CT imaging; either as a screening tool regardless of disease stage ($n=47$) or to further characterize known panNETs ($n=11$). SSTR PET/CT and matched conventional imaging were blindly analyzed. We assessed the findings and the impact of SSTR PET/CT during a median follow-up of 47 months.

Results: SSTR PET/CT detected three times as many panNETs as conventional imaging ($P<.001$). SSTR PET/CT altered the management of 27 patients (47%). Seven patients (12%) were referred for surgery, and five (9%) received systemic treatment. In 15/25 (60%) patients with no previous panNET ($n=22$) or in remission after surgery ($n=3$), SSTR PET/CT identified a panNET ($n=14$) or recurrence ($n=1$). In eight patients, SSTR PET/CT revealed a panNET not immediately visible on conventional imaging. During a median follow-up of 47 months, three became visible on conventional imaging, but none required intervention. When SSTR PET/CT was negative, no panNETs were identified on conventional imaging during 38 months of follow-up.

Conclusions: SSTR PET/CT demonstrates high accuracy in the detection of panNETs and alters the clinical management in nearly half of the MEN1-patients. SSTR PET/CT enables timely diagnosis and staging of MEN1-related panNETs.

Keywords: MEN1, pancreas, NET, pancreatic neuroendocrine tumor, somatostatin receptor PET/CT

Significance

The role of somatostatin receptor positron emission tomography/computed tomography (SSTR PET/CT) in the follow-up of pancreatic neuroendocrine tumors (panNETs) in multiple endocrine neoplasia type 1 (MEN1) has not been established. This study shows that SSTR PET/CT detects three times as many panNETs as conventional imaging and alters the clinical management of 47% of patients. SSTR PET/CT identifies small panNETs not visible on control conventional imaging that do not demonstrate clinically significant growth during four-year conventional imaging follow-up. When SSTR PET/CT imaging was negative, neither magnetic resonance imaging nor CT detected any panNETs during the three-year follow-up. Long follow-up and blinded imaging analysis enabled us to pinpoint situations in which the interventions were specifically attributable to SSTR PET/CT. Our findings may help tailor the imaging follow-up of MEN1.

Received: February 3, 2023. Revised: March 2, 2023. Accepted: March 13, 2023

© The Author(s) 2023. Published by Oxford University Press on behalf of European Society of Endocrinology.

This is an Open Access article distributed under the terms of the Creative Commons Attribution License (<https://creativecommons.org/licenses/by/4.0/>), which permits unrestricted reuse, distribution, and reproduction in any medium, provided the original work is properly cited.

Introduction

Well-differentiated neuroendocrine tumors frequently express somatostatin receptors (SSTRs) on their cell surface, enabling the use of radiolabeled SSTR-binding ligands for the imaging of pancreatic neuroendocrine tumors (panNETs).^{1,2} Because of its high sensitivity and spatial resolution, SSTR positron emission tomography with low-dose computed tomography (CT) [SSTR positron emission tomography/CT (SSTR PET/CT)] has been successfully implemented in diagnosing and staging sporadic noninsulinoma panNETs.³⁻⁵ In multiple endocrine neoplasia type 1 (MEN1) syndrome, decreased life expectancy is related to NETs, with panNETs constituting the leading cause of death.^{6,7}

The timely detection of potentially aggressive nonfunctioning panNETs before the development of metastases forms the cornerstone of the follow-up. In MEN1, chromogranin A and pancreatic polypeptide have a low diagnostic value for detecting nonfunctioning panNETs.⁸⁻¹⁰ As such, diagnostics rely on imaging studies. Surgical treatment is recommended for tumors ≥ 2 cm in diameter and for smaller rapidly growing tumors.¹¹

Contemporary guidelines recommend screening and follow-up of panNETs with either magnetic resonance imaging (MRI), endoscopic ultrasound (EUS), or CT.^{11,12} MRI and CT suffer from reduced sensitivity, especially with smaller lesions. Although EUS has been considered the most sensitive imaging method, it is invasive, operator dependent, and subject to availability.¹³ Because of the limitations of conventional imaging, there is an unmet need for novel diagnostic imaging tools. Although SSTR PET/CT has been recognized as a sensitive imaging tool in patients with MEN1, its role in screening and follow-up has yet to be established.^{8,14,15}

Only a few studies with a limited patient population have assessed the performance of SSTR PET/CT as a pancreatic imaging tool in MEN1.¹⁶⁻²² In their cross-sectional study including 19 MEN1 patients, Morgat et al.¹⁶ investigated duodenopancreatic NETs with SSTR PET/CT, SSTR scintigraphy, and CT, reporting that SSTR PET/CT detected significantly more pancreatic lesions than conventional imaging. Patil et al.¹⁷ described 34 MEN1 patients who underwent SSTR PET/CT in a retrospective setting. When SSTR PET/CT was used in conjunction with multiphase contrast-enhanced CT, the combined use of imaging modalities detected significantly more gastroenteropancreatic lesions and metastases than CT alone. Lastoria et al.¹⁸ described 18 MEN1 patients, in whom SSTR PET/CT identified all pancreatic lesions on various conventional imaging modalities, reporting a sensitivity of 100%.

According to studies assessing the clinical impact of SSTR PET/CT in MEN1 (Mennetrey, Sadowski, Froeling),²⁰⁻²² the proportion of patients with reported benefit varied between 31% and 48%. However, Albers et al.¹⁹ prospectively studied 33 MEN1 patients whose follow-up, including EUS, abdominal MRI, and thoracic CT, was supplemented with SSTR PET/CT. Unlike the previously mentioned studies, conventional imaging overperformed SSTR PET/CT in detecting panNETs; however, SSTR PET/CT discovered additional, but clinically nonsignificant, lymph node ($n = 3$) and liver metastases ($n = 4$).

The aim of the present study was to compare the performance and value of SSTR PET/CT compared with conventional pancreatic imaging in the management of patients with MEN1

in a real-life setting. We evaluated these modalities in different clinical situations: as a screening tool for all MEN1 patients, regardless of current disease stage, and as a staging tool in patients with known panNETs only.

Patients and methods

Study design

We evaluated the performance of SSTR PET/CT compared with conventional pancreatic imaging among MEN1 patients treated at the Helsinki (cohort A) and Turku (cohort B) University Hospitals during the years 2013-2021. Patient characteristics, disease manifestations, laboratory results, surgery, pathology reports, and data on possible other interventions were gathered from the electronic patient records. Laboratory parameters were analyzed using in-house methods in the respective hospitals. Because of the methodological changes in some diagnostic tests over time, all laboratory data are presented as a percentage of the upper limit of normal.

Patients

At Helsinki University Hospital, SSTR PET/CT was introduced as a routine one-time screening tool for all patients, regardless of disease stage, in 2018. All MEN1 patients ($n = 47$, cohort A) were prospectively screened with SSTR PET/CT using a local follow-up protocol, the primary aim being the detection and staging of possible panNETs. At Turku University Hospital, all patients had been previously diagnosed with panNET ($n = 11$, cohort B) and underwent SSTR PET/CT to further characterize the tumor. The findings were retrospectively analyzed. Seven of these patients were previously described by Majala et al.²³

In the present study, 11 patients (19%) had undergone surgery for panNET before SSTR PET/CT imaging. Two (18%) patients had undergone total pancreatectomy, six (55%) partial resection of the pancreas, and three (27%) tumor enucleation.

The study was performed in accordance with the Declaration of Helsinki. Authorization to perform this study without individual consent was granted by the institutional review boards of Helsinki University Hospital (HUS/115/2020) and Turku University Hospital (T03/011/21).

Imaging protocols and analysis of imaging data

Whole-body PET/CT images from the vertex to mid-thigh were acquired after an intravenous injection of ~ 1.5 - 2 MBq/kg of ⁶⁸Gallium-DOTANOC and 60-min rest.

Three different PET/CT systems were used: Philips Gemini GXL 16 (Philips Healthcare, MA, USA), Siemens Biograph mCT Flow 64 (Siemens Healthcare, IL, USA), and GE Discovery MI 128 (General Electric Healthcare, WI, USA). The pixel size was 2.7×2.7 or 4×4 mm, slice thickness 2.8 to 5 mm, and imaging time/bed position 2.5-3 min.

Attenuation correction was made with a low-dose CT, which was used for anatomical localization. No contrast medium was used. One patient underwent concurrent MRI for anatomical localization.

The conventional imaging of the upper abdomen was conducted by MRI in 51 patients and CT in seven patients. MRI imaging was conducted with either 1.5- or 3-T high-field MRI. For one patient, only magnetic resonance cholangiopancreatography

(MRCP) and T2-weighted anatomical imaging were available. For all other patients, the MRI protocol included gadolinium-enhanced T1-weighted fat-saturated sequences in at least the arterial and venous phases in the axial plane, a T1 fat-saturated axial sequence without contrast in all but one patient, anatomical T2-weighted sequences in the axial and coronal planes, and diffusion-weighted imaging in the axial plane. In most patients, MRCP sequences were obtained.

CT imaging was conducted with helical acquisition, and the three-dimensional data set was reconstructed into 3-mm slices in the axial, coronal, and sagittal planes. For three patients, the CT protocol included both arterial and venous phases of the upper abdomen; for one patient, only the arterial phase was available; and for another, only the venous phase was available.

Comparison of PET/CT data to conventional imaging

The available SSTR PET/CT results were compared with conventional MRI or CT results. Conventional imaging performed in the closest vicinity to the SSTR PET/CT [median difference 3.0 months, interquartile range (IQR) 1.2–7.8] was chosen for comparison. In 33 (57%) patients, SSTR PET/CT was performed after the conventional imaging used for comparison. No anatomy-altering surgery was allowed between the images used in the analysis.

SSTR PET/CT and conventional imaging results were reanalyzed in a blinded fashion by two independent experts (HP and JS), and the detected lesions were compared. For discordant head-to-head imaging results between modalities, further analysis of specific lesions was undertaken. In these cases, evaluation was based on follow-up including further imaging (median follow-up 49 months, IQR 30–64).

Impact of SSTR PET/CT on patient management

The real-life clinical impact of SSTR PET/CT imaging was assessed by the investigators using available follow-up data from electronic patient records, including imaging, surgical, histopathological outcomes, and changes in systemic treatments. Histopathological confirmation of panNET detected on imaging during the present study was available from 13 patients. Eleven of the specimens were from surgical removal of the tumor, and two from EUS facilitated biopsy. The median follow-up was 47 months (IQR 29–66).

The clinical impact was categorized as no change in follow-up scheme, intensified follow-up, referral for surgery, or other intervention. The disease stage at the time of SSTR PET/CT imaging was categorized as: (1) screening (no previous diagnosis of panNET), (2) staging (follow-up of untreated panNET), (3) restaging (previous treatment for panNET), or (4) evaluation for suitability of peptide receptor radionuclide therapy (PRRT). The categorization was adapted from Mennetrey *et al.*²⁰ After categorization, patients in cohorts A/B were classified as follows: 20/0 (34%/0%) to screening, 16/10 (28%/91%) to staging, 10/0 (17%/0%) to restaging, and 1/1 (2%/9%) to evaluation for suitability for PRRT.

Statistical analysis

Statistical analysis was performed using IBM SPSS 25 (IBM Corp., Armonk, NY, USA), except for Kaplan–Meier estimate, which was performed using R 4.2.1 (R Core Team

2022). Data are presented as means and standard deviations, medians and either IQR, or ranges for continuous variables. The categorical variables are presented as frequencies and proportions. Continuous variables were compared using a *t*-test or Mann–Whitney *U* test in case of a non-normal distribution. Categorical variables were compared using the chi-squared test. The reported *P*-values are two-sided, with a *P*-value of <.05 considered statistically significant.

Results

Patient characteristics

The clinical characteristics and biochemistry of the 58 patients with MEN1 syndrome are presented in [Table 1](#). Cohort A comprised 47 patients (median age at SSTR PET/CT 39 years, range 16–72 years), and cohort B comprised 11 patients (median age at SSTR PET/CT 40 years, range 20–68 years). Diagnosis of MEN1 was confirmed with genetic testing in all but one patient, whose diagnosis was clinical. The Kaplan–Meier estimate of age at time of the first diagnosis of panNET is shown in [Figure 1](#).

Imaging

Pancreatic, liver, and lymph node lesions detected on blinded evaluation of SSTR PET/CT and conventional imaging

Pancreatic lesions. The imaging findings are described in [Table 2](#). Compared with conventional imaging, SSTR PET/CT detected significantly more NET lesions in the pancreas. This was true for the entire pancreas ($P < .001$) and for both the head ($P < .001$) and body-tail ($P = .001$) regions. SSTR PET/CT imaging detected significantly more patients with at least one panNET in the entire pancreas ($P = .002$), head ($P < .001$), and body-tail ($P = .005$) regions. The performance difference of conventional imaging modalities (MRI and CT) compared with SSTR PET/CT was similar ($P = .16$, data not shown).

Liver lesions. There was no statistically significant difference in the amount of suspected liver metastases (13 vs. 23, $P = .54$) or the proportion of patients with suspected liver metastases (12% vs. 16% $P = .59$) between the SSTR PET/CT and conventional imaging modalities ([Table 2](#)).

Lymph node lesions. SSTR PET/CT detected lymph node metastases not identified on conventional imaging in four patients; three of these metastases were in the abdominal and one in the mediastinal region. Two of the patients underwent surgery, and histopathology confirmed NET tissue.

Paired patient-matched comparison of SSTR PET/CT and conventional imaging

Pancreatic lesions. On average, SSTR PET/CT detected 1.53 (± 2.19) more panNETs per patient than conventional imaging. The distribution of additional panNETs detected is shown in [Figure 2](#). The mean difference was 0.67 (± 1.1) and 0.86 (± 1.5) for the head and body-tail regions, respectively. The ability of SSTR PET/CT to detect additional lesions was similar for the head and body-tail regions ($P = .44$).

For the assessment of none versus any panNET, SSTR PET/CT and conventional imaging did not align in 20/58 (34%) patients. The paired comparative results of SSTR PET/CT and

Table 1. Baseline patient characteristics.

Variable	All patients (n = 58)	Cohort A (n = 47)	Cohort B (n = 11)
Sex, female/male (n)	30/28 (52%/48%)	23/24 (49%/51%)	7/4 (64%/36%)
Basis of MEN1-diagnosis			
Confirmed gene defect (n)	57 (98%)	47 (100%)	10 (91%)
Clinical diagnosis (n)	1 ^a (2%)	0 (0%)	1 ^a (9%)
Age at diagnosis of MEN1 (years)	28 (19-47)	28 (19-47)	31 (24-41)
Diagnosis of panNET before SSTR PET/CT imaging (n)	36 (62%)	25 (53%)	11 (100%)
Previous surgical treatment for panNET (n)	11 (19%)	10 (21%)	1 (9%)
Somatostatin analog treatment (n)	8 (14%)	6 (13%)	2 (18%)
Age at SSTR PET/CT imaging (years)	40 (28-56) [16-72]	39 (28-57) [16-72]	42 (35-47) [20-68]
Conventional imaging modality used for comparison			
Magnetic resonance imaging (n)	51 (88%)	41 (87%)	10 (91%)
Computed tomography (n)	7 (12%)	6 (13%)	1 (9%)
Laboratory parameters at SSTR PET/CT imaging			
Chromogranin A (% of upper limit of normal)	92 (70-154)	90 (70-132)	125 (77-187)
Pancreatic polypeptide (% of upper limit of normal)	65 (24-183)	42 (24-76)	205 (26-350)
Gastrin (% of upper limit of normal)	25 (18-64)	24 (18-63)	42 (25-51)

Data are presented as median (interquartile range)/[range] or frequency (proportion), as appropriate.

Abbreviations: MEN1, multiple endocrine neoplasia type 1; panNET, pancreatic neuroendocrine tumor; SSTR PET/CT, somatostatin receptor positron emission tomography/computed tomography.

^aClinical diagnosis was based on occurrence of panNET, primary hyperparathyroidism, pituitary adenoma, and adrenal adenoma.

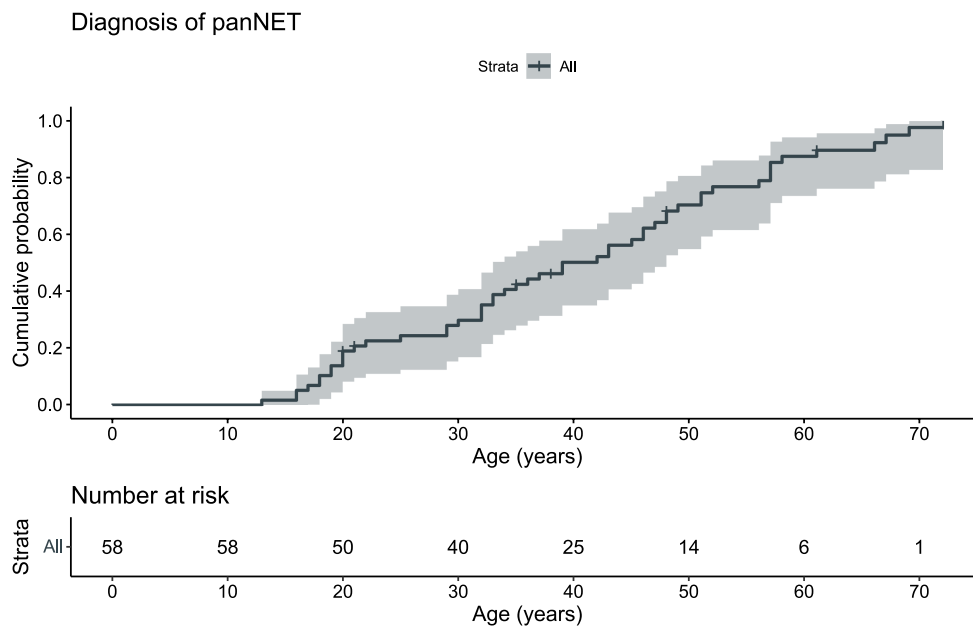


Figure 1. Kaplan–Meier survival estimate for the first-time diagnosis of pancreatic neuroendocrine tumor (panNET) in a MEN1 population that has undergone SSTR PET/CT imaging. 95% confidence interval in gray. Crosses imply censored data. To provide relevant epidemiological data, cohort B was omitted from the analysis to address selection bias related to all patients in the cohort having previous panNET diagnosis.

conventional imaging are shown in Table 3. In 18 patients, lesions detected by SSTR PET/CT were not visible on conventional imaging. In two patients, conventional imaging displayed a lesion, while SSTR PET/CT displayed none. In addition, in two patients, conventional imaging demonstrated additional pancreatic lesions compared with those detected by SSTR PET/CT.

Liver lesions. Six patients (10%) displayed discordant results. In four cases, metastases were suspected on conventional imaging but not on SSTR PET/CT. In two cases, metastases were suspected on SSTR PET/CT but not on conventional imaging.

Further evaluation of discordant pancreatic imaging results

Four patients had discrepant results in which conventional imaging displayed more suspected panNETs. In a 49-year-old patient, a 27-mm pancreatic tumor was identified on MRI but was not visible on SSTR PET/CT. The patient underwent pancreatoduodenectomy, and histopathology confirmed pancreatic adenocarcinoma. In a 64-year-old patient, SSTR PET/CT demonstrated one but CT two possible panNETs. Histopathology confirmed the SSTR PET/CT positive lesion to be a panNET; the other tumor detected on CT was a microadenoma. In a 72-year-old patient, CT demonstrated a hyper-vascular NET lesion in the uncinate region of the pancreas,

Table 2. Lesions detected by imaging modality.

Organ	Total number of lesions			Number of patients with at least one lesion		
	SSTR PET/CT	Conventional imaging (MRI/CT)	<i>P</i> -value	SSTR PET/CT	Conventional imaging (MRI/CT)	<i>P</i> -value
Pancreas						
Total	133	44	<.001	47 (81%)	31 (53%)	.002
Head	50	10	<.001	31 (53%)	8 (14%)	<.001
Body/tail	83	34	.001	39 (67%)	24 (41%)	.005
Liver	13	23	.54	7 (12%)	9 (16%)	.59

Abbreviations: CT, computed tomography; MRI, magnetic resonance imaging; SSTR PET/CT, somatostatin receptor positron emission tomography/computed tomography.

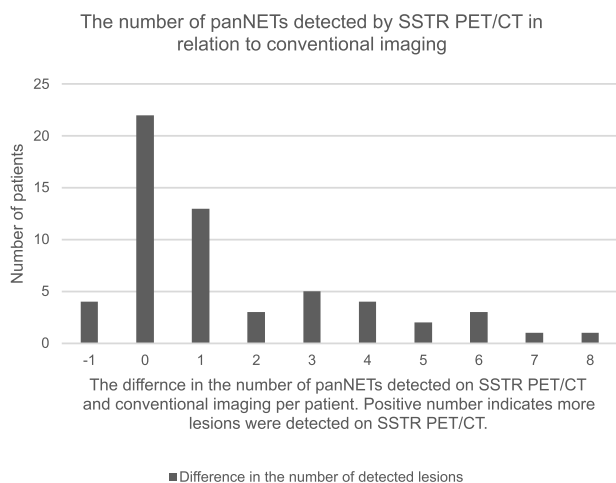


Figure 2. The difference in the number of detected pancreatic neuroendocrine tumors (panNETs) in patient-matched paired analysis of SSTR PET/CT and conventional imaging. The number of panNETs detected by conventional modalities is subtracted from the number of SSTR PET/CT detected panNETs.

while the corresponding SSTR PET/CT uptake was interpreted to be physiological. In response to PRRT, this lesion decreased in size on conventional imaging. The fourth patient, a 32-year-old individual, had three panNETs on MRI but only two on SSTR PET/CT. Thirty months of follow-up with MRI confirmed two to be a true positive.

Assessment of discordant liver imaging results

Six patients had discordant imaging results for suspected liver metastases. In four cases, metastases were suspected on conventional but not on SSTR PET/CT imaging. Three of these cases (33-year-old, 38-year-old, and 60-year-old patients) were false positive MRI findings that could be explained by abnormal hepatic perfusion. In the fourth case, CT demonstrated widespread liver metastases in a 45-year-old patient (images displayed in Figure 3). Liver biopsy confirmed thyroid transcription factor 1 expressing NET tissue compatible with pulmonary origin. In addition, SSTR PET/CT was positive in two cases, but corresponding lesions were not detected on MRI. In the first case, a 24-year-old patient, a tracer-positive lesion was first interpreted as segment III liver metastasis. Additional imaging and clinical follow-up confirmed a panNET located in the body of the pancreas. In the second case, SSTR PET/CT detected a panNET liver metastasis in a 20-year-old patient, and the diagnosis was confirmed by biopsy.

Table 3. Patient-matched comparison of SSTR PET/CT and conventional imaging results.

Any suspected pancreatic NET	MRI/CT+	MRI/CT-
SSTR PET/CT +	29 (50%)	18 (31%)
SSTR PET/CT -	2 (3%)	9 (16%)
Any suspected liver metastases	MRI/CT+	MRI/CT-
SSTR PET/CT +	5 (9%)	2 (3%)
SSTR PET/CT -	4 (7%)	47 (81%)

Abbreviations: CT, computed tomography; MRI, magnetic resonance imaging; SSTR PET/CT, somatostatin receptor positron emission tomography/computed tomography.

Real-life clinical impact of SSTR PET/CT imaging

SSTR PET/CT imaging altered the management of 27/58 (47%) patients. In the majority ($n = 15$), this was because of novel discoveries requiring further characterization or more frequent follow-up. Twelve patients received further treatments, either referrals to surgery ($n = 7$) or other interventions ($n = 5$). Half of the interventions ($n = 6$) were because of discoveries not related to panNETs. The patients who received further treatments are described in Table 4. The clinical impact by disease stage is described in Table 5.

Clinical significance of new panNETs detected by SSTR PET/CT

Overall, 25 patients were at risk for novel panNET diagnosis, either having no prior diagnosis ($n = 22$) or having received curative surgery ($n = 3$), excluding patients who had undergone pancreatectomy. In this group, SSTR PET/CT screening identified novel panNETs in 14 patients and one recurrence in a patient who had undergone curative surgery for panNET 7.8 years earlier.

On immediate conventional imaging follow-up, the corresponding lesion was identified in seven (47%) patients, five on MRI, and two on CT. Two of these panNETs were ≥ 2 cm in diameter and, thus, referred for surgery. In eight (53%) patients, no corresponding lesions were identified immediately. Further conventional imaging follow-up during a median of 37 months (range 13-84) revealed anatomical lesions in 3/8 (38%) patients, two with CT and one with MRI. None of these lesions were ≥ 2 cm or demonstrated rapid growth. The median follow-up with conventional imaging in patients without panNETs was 28 months. When SSTR PET/CT was negative at baseline, no panNETs were detected on conventional imaging after a median follow-up of 38 months. The events in clinical follow-up after SSTR PET/CT imaging in a population at risk for novel panNET diagnosis are shown in Figure 4.

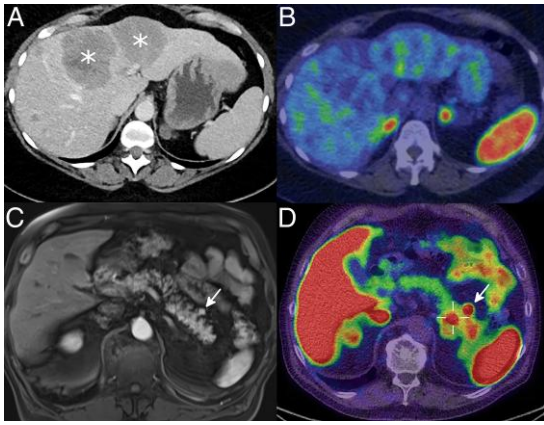


Figure 3. Patient-matched comparative images of conventional imaging and SSTR PET/CT. Top row: A: On the left, computed tomography images of the venous phase displaying two large hypovascular metastatic masses marked with white asterisks. Histopathology confirmed NET tissue with likely pulmonary origin. B: On the right, these metastases did not exhibit tracer uptake on SSTR PET/CT. Bottom row: D: SSTR PET/CT image on the right displaying two adjacent pancreatic neuroendocrine tumors in the tail of pancreas (one marked with white arrow, other surrounded by white crosshairs). On the left, C: only one corresponding tumor could be seen on the magnetic resonance images, marked with a white arrow.

Discussion

The present study has provided detailed novel insights into the role of SSTR PET/CT as a screening and staging/restaging tool in pancreatic imaging among MEN1 patients. The strengths of the study include blinded analysis of imaging data, relatively large patient sample, and a follow-up of almost four years, including regular conventional pancreatic imaging surveillance, enabling assessment of discordant imaging results, and overall clinical impact. A limitation is the partially retrospective design of the study, which can lead to bias and reduce overall representativeness of our data. Overall, SSTR PET/CT detected significantly more panNETs than conventional imaging with either MRI or CT. These results are in line with most previous studies comparing SSTR PET/CT to conventional imaging modalities. SSTR PET/CT detected panNETs in 30% of patients without corresponding lesions on conventional imaging and was found to impact clinical management in 47% of the patients in our MEN1 series.

SSTR PET/CT screening led to first-time diagnosis of panNET ($n=14$) or recurrence ($n=1$) in 15/25 patients (60%) at risk for new panNET diagnosis. Three of these patients were under 20 years old. During a median follow-up of nearly four years with standard conventional pancreatic imaging, none of the newly detected panNETs that were not immediately visible on conventional imaging required interventions. Other studies utilizing SSTR PET/CT in MEN1 have not presented the follow-up results of newly discovered panNETs. Our results suggest that novel SSTR PET/CT detected panNETs that are not immediately visible on MRI/CT do not necessarily need intense follow-up but might instead be tailored for next conventional pancreatic imaging three to five years later. However, future studies that include more MEN1 patients are still needed to answer this question. Additionally, when SSTR PET/CT imaging was negative, standard conventional imaging surveillance during the three-year follow-up did not reveal any panNETs. Current

guidelines recommend pancreatic imaging <10 years of age,²⁴ however Klein Hanevald et al.²⁵ concluded that 13-14 years is justified. Taken together, in the future, in adult MEN1 patients (≥ 18 years), SSTR PET/CT screening for the detection of panNETs could be recommended for all, and in children, from the age of 13-15 years.

Most studies utilizing SSTR PET/CT among MEN1 patients have reported discoveries of additional lymph node metastases.^{16,17,19,22} Importantly, Mennetrey et al. demonstrated that SSTR PET/CT identified lymph node metastases already at screening in 21% of the patients, with conventional imaging displaying significantly inferior performance.²⁰ The discovery of additional lymph node metastases is repeated in our study, with four patients having metastases on SSTR PET/CT, while none of them were visible on conventional imaging. In one case, the diagnosis prompted radical surgery of the primary tumor and local metastasis. The detection of a locally advanced disease can be of benefit because curative radical surgery may be feasible in locally advanced panNET in MEN1.²⁶ Conventional imaging modalities appear to have a limited ability to distinguish lymph node metastases when compared with SSTR PET/CT. As more evidence accumulates, SSTR PET/CT imaging could enable tailored imaging follow-up, with the aim of reducing the burden for both the patient and health care system, still enabling the timely discovery of panNETs that should undergo resection, and small, aggressive panNETs that have already metastasized.

It is noteworthy that Albers et al.¹⁹ found conventional surveillance of MEN1 patients with EUS and abdominal MRI to be superior to SSTR PET/CT. In the studies by Lastoria et al.¹⁸ and Mennetrey et al.,²⁰ 16/18 (89%) and 40/108 (37%) MEN1 patients, respectively, also underwent EUS. In these studies, for detection of panNETs in a patient-matched setting, the performance of EUS and SSTR PET/CT was similar. However, EUS and SSTR PET/CT are not available in all centers, and patients with MEN1 may not necessarily benefit from undergoing both investigations. It seems plausible that EUS and SSTR/PET CT could serve as complimentary tools according to their availability because both reportedly demonstrate improved sensitivity compared with conventional imaging in detecting panNETs.^{11,16-18} Of note, heavy investigational protocols burden the patients, and accurate diagnostics may affect the health-related quality of life in patients with MEN1.²⁷

A strength of the present study was the substantial median follow-up (49 months), which enabled us to assess discordant imaging results. Based on this, SSTR PET/CT was correct in at least 7/10 discordant cases when assessing MEN1-related lesions. In four patients, panNET was suspected on conventional imaging but not on SSTR PET/CT. Of these, the follow-up confirmed three false positives of conventional imaging for panNET (MRI = 2, CT = 1), one of which was a pancreatic adenocarcinoma and, thus, clinically significant. Pancreatic adenocarcinomas have been previously reported in patients with MEN1.²⁸ The last discordant result was possibly a false negative SSTR PET/CT, where conventional imaging (CT) suspected panNET in the uncinate region of pancreas. The high background tracer uptake²⁹ was interpreted as physiological. During further follow-up, the suspected lesion shrank in response to PRRT, suggesting that the lesion was a panNET. Of the discordant liver lesions, SSTR PET/CT was accurate in 4/6 cases. One false positive was because of the misallocation of panNET tracer uptake into the liver, which was attributable to a breathing-related artifact. An additional

Table 4. Clinical details of patients who underwent interventions following SSTR PET/CT imaging.

Patient	Alteration in clinical management	Lesion responsible for the alteration of clinical management	Description of clinical details
1	Referral for surgical treatment	Novel tracer-positive abdominal lymph node not visualizing on MRI	Distal pancreatectomy (four tracer-avid panNETs and positive lymph node). Histopathology confirmed panNET diagnoses and NET tissue in the lymph node
2	Referral for surgical treatment	Novel ≥ 2 cm panNET	The patient had no previous diagnosis of panNET. With the SSTR PET/CT data available, the panNET was retrospectively identified also on the MRI series dating eight years back. Histopathology from EUS-assisted biopsy confirmed the diagnosis. Of note, the panNET was identified on blinded analysis of MRI images of the present study
3	PRRT	Tracer positivity of liver NET metastases	Advanced disease and strong SSTR uptake led to initiation of PRRT.
4	Referral for surgical treatment	Novel ≥ 2 cm panNET	SSTR PET/CT as the first-time abdominal imaging, primary discovery of panNET, also visualized (2.0 cm) on concomitant MRI. Histopathology confirmed the diagnosis. Of note, the panNET was identified on blinded analysis of MRI images of the present study
5	Initiation of other systemic treatment	Novel breast cancer metastasis	Discovery of novel bone metastasis in ilium led to change in systemic treatment of breast cancer
6	Referral for surgical treatment	Tracer-positive lung lesion	Corresponding lesion could be seen on thoracic CT. Histopathology confirmed the diagnosis of well-differentiated lung NET.
7	Referral for surgical treatment	Novel tracer-positive solitary liver metastasis not visualizing on MRI	After follow-up of a stable disease, the patient underwent resection of primary panNET and liver metastasis. Histopathology confirmed the diagnosis of panNET and NET-metastasis
8	Referral for surgical treatment	Novel tracer-positive retroperitoneal lesion not visualizing on MRI	Patient had gastrointestinal symptoms and elevated gastrin levels; both resolved after surgical removal of the lesion. Histopathology confirmed NET diagnosis
9	Referral for surgical treatment	Confirmation of suspected NET diagnosis by SSTR PET/CT	SSTR PET/CT confirmed panNET diagnosis. Surgical treatment was opted in because of patient-related reasons, even though tumor size was below surgical threshold regarding size and growth rate. Histopathology confirmed the diagnosis of panNET
10	Initiation of somatostatin analog	Novel tracer-positive liver metastases	Initiation of somatostatin analog treatment. The lesion is thought to originate from previously treated duodenal NET. Of note, the liver metastasis was seen on blinded analysis of MRI images of the present study
11	Initiation of other systemic treatment	Tracer negativity of liver metastases of NET	Widely advanced disease led to the initiation of temozolomide treatment. Based on histology, the metastases are thought to originate from lung NET
12	Initiation of somatostatin analog	Novel tracer-positive lymph node lesions not visualizing on MRI	Initiation of somatostatin analog treatment. The lesion is thought to originate from previously treated duodenal NET

Abbreviations: CT, computed tomography; EUS, endoscopic ultrasound; MRI, magnetic resonance imaging; NET, neuroendocrine tumor; panNET, pancreatic neuroendocrine tumor; PRRT, peptide receptor radionuclide therapy; SSTR PET/CT, somatostatin receptor positron emission tomography/computed tomography.

Table 5. Clinical impact of SSTR PET/CT imaging on the follow-up and management of patients stratified by the previous panNET history.

	Screening ($n = 20$) ^a	Staging ($n = 26$) ^b	Restaging ($n = 10$) ^c	PRRT assessment ($n = 2$) ^d
Continuation of previous follow-up scheme	5	18	8	0
Intensified follow-up	12	2 (1)	1	0
Referral for surgical treatment	2	4 (1)	1 (1)	0
Other intervention	1 (1)	2 (2)	0	2 (1)

The number of alterations that were attributable to non-panNET discoveries is shown in brackets.

^aNo previously detected pancreatic neuroendocrine tumor (panNET).

^bFollow-up of untreated panNET.

^cPrevious treatment for panNET.

^dEvaluation for suitability of peptide receptor radionuclide therapy (PRRT).

false negative was because of true liver metastatic NET tissue of likely pulmonary origin not exhibiting tracer uptake.

In line with conventional CT, SSTR PET/CT has been criticized for its high ionizing radiation burden and, thus, considered unsuitable for MEN1 tumor screening.¹⁵ However, this must be balanced against the risk of potential delayed diagnosis of NET or metastasized disease. In Helsinki University Hospital, the radiation dose of SSTR PET/CT is 4.5-7.0 mSv, which compares favorably to multiphasic

contrast-enhanced abdominal CT, here with a reported dose of ~ 13 mSv.³⁰ Implementation of time-of-flight PET technology can provide even further reductions in radiation exposure.³¹

SSTR PET/CT led to changes in clinical management in 47% of the patients, with half of the changes attributable to novel panNET discoveries requiring intensified follow-up. In addition, 12% of the patients were referred for surgical intervention, and 9% received systemic treatment. Although many

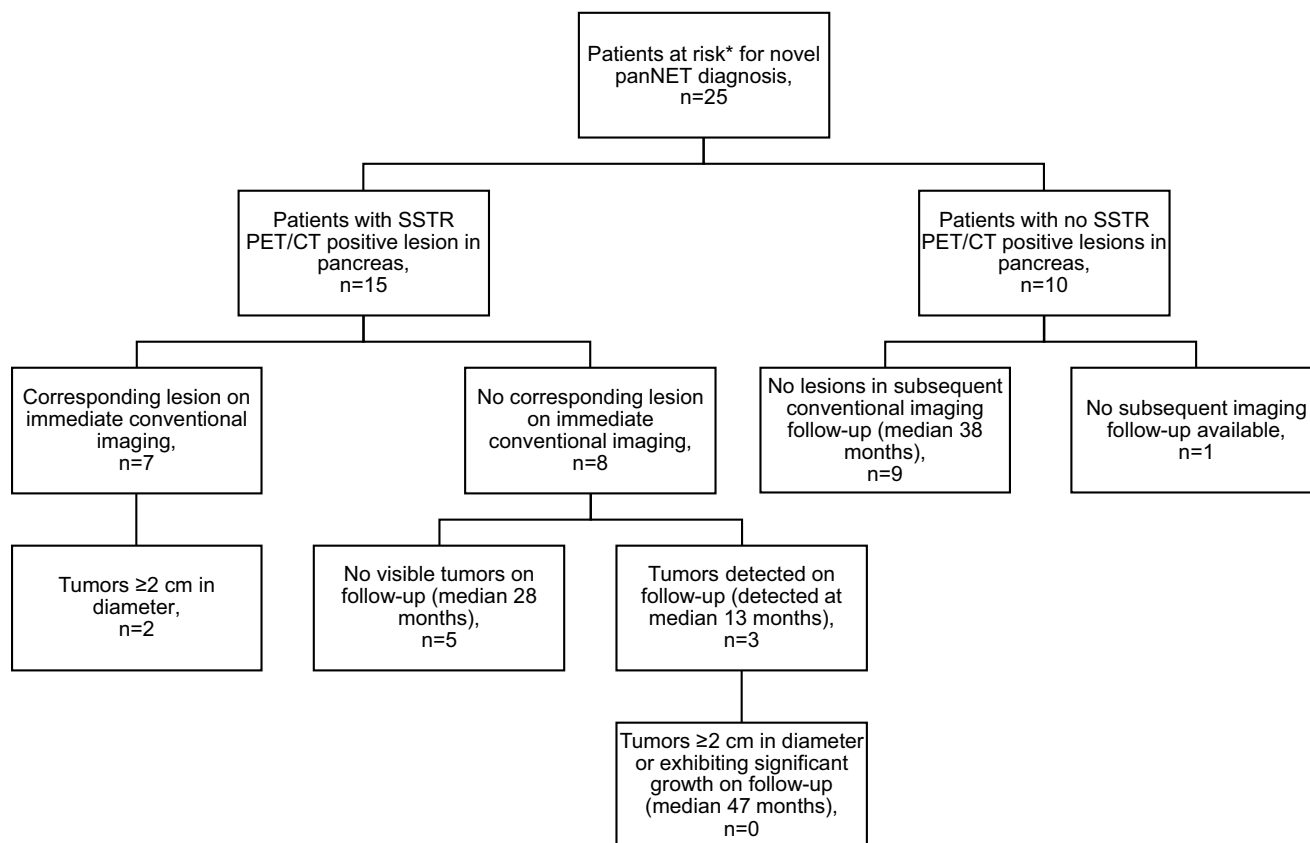


Figure 4. Flowchart of the clinical follow-up results of patients without previous diagnosis of panNET or preceding curative surgery with clinical remission, that is, patients at risk for novel panNET diagnosis. *Patients at risk included 22 patients who had no prior diagnosis of pancreatic neuroendocrine tumor (panNET) and three patients who had received curative surgery for panNET with no other known panNETs. Patients with previous pancreatectomy were not considered at risk.

of the interventions could have been reached with conventional imaging modalities, based on the available follow-up data and blinded imaging analysis, SSTR PET/CT specifically enabled tumor surgery with curative aims for three patients. Previous studies have reported comparable levels of influence of SSTR PET/CT in the clinical management of patients (31%-48%), while the rate of surgery has been higher (27%-43%).^{21,22,32} Previous studies have not provided enough data to assess whether conventional imaging could have provided comparable results to SSTR PET/CT in subsequent clinical follow-up.

In summary, the SSTR PET/CT imaging of MEN1 patients was able to detect a significantly larger number of panNETs compared with conventional imaging, altering the clinical management in almost half of the patients. SSTR PET/CT imaging enables the timely diagnosis and staging of MEN1-related panNETs.

Funding

This work was supported by Finska Läkaresällskapet (I.K. and C.S.-J.) and Helsinki University Hospital research grants (grant TYH2020334 to C.S.-J.).

Author contribution

Concept and study design: I.K., H.P., J.S., E.M.R., C.S.-J. Data acquisition: I.K., S.M., H.P., E.M.R., J.S. Statistical analysis: I.K. Interpretation of results: I.K.,

E.M.R., N.M., C.S.-J. Original draft of manuscript: I.K., E.M.R., N.M., C.S.-J. Figures: I.K., H.P., J.S. Coordination and administration: I.K., E.M.R., S.M., C.S.-J. Critical review and editing of the final manuscript: I.K., S.M., J.S., H.P., S.K., H.S., P.J.M., N.M., E.M.R., C.S.-J.

Conflicts of interest: None declared.

References

1. Reubi JC. Regulatory peptide receptors as molecular targets for cancer diagnosis and therapy. *Q J Nucl Med.* 1997;41(2):63-70.
2. Bozkurt MF, Virgolini I, Balogova S, *et al.* Guideline for PET/CT imaging of neuroendocrine neoplasms with 68Ga-DOTA-conjugated somatostatin receptor targeting peptides and 18F-DOPA. *Eur J Nucl Med Mol Imaging.* 2017;44(9):1588-1601. <https://doi.org/10.1007/s00259-017-3728-y>
3. Falconi M, Eriksson B, Kaltsas G, *et al.* ENETS consensus guidelines update for the management of patients with functional pancreatic neuroendocrine tumors and non-functional pancreatic neuroendocrine tumors. *Neuroendocrinology.* 2016;103(2):153-171. <https://doi.org/10.1159/000443171>
4. Janson ET, Knigge U, Dam G, *et al.* Nordic guidelines 2021 for diagnosis and treatment of gastroenteropancreatic neuroendocrine neoplasms. *Acta Oncol.* 2021;60(7):931-941. <https://doi.org/10.1080/0284186X.2021.1921262>
5. Sundin A, Arnold R, Baudin E, *et al.* ENETS consensus guidelines for the standards of care in neuroendocrine tumors: radiological, nuclear medicine & hybrid imaging. *Neuroendocrinology.* 2017;105(3):212-244. <https://doi.org/10.1159/000471879>

6. Goudet P, Murat A, Binquet C, *et al.* Risk factors and causes of death in MEN1 disease. A GTE (Groupe d'Etude des Tumeurs Endocrines) cohort study among 758 patients. *World J Surg.* 2010;34(2):249-255. <https://doi.org/10.1007/s00268-009-0290-1>
7. Ito T, Igarashi H, Uehara H, Berna MJ, Jensen RT. Causes of death and prognostic factors in multiple endocrine neoplasia type 1: a prospective study: comparison of 106 MEN1/Zollinger-Ellison syndrome patients with 1613 literature MEN1 patients with or without pancreatic endocrine tumors. *Medicine (Baltimore).* 2013; 92(3):135-181. <https://doi.org/10.1097/MD.0b013e3182954af1>
8. Al-Salameh A, Cadiot G, Calender A, Goudet P, Chanson P. Clinical aspects of multiple endocrine neoplasia type 1. *Nat Rev Endocrinol.* 2021;17(4):207-224. <https://doi.org/10.1038/s41574-021-00468-3>
9. de Laat JM, Pieterman CRC, Weijmans M, *et al.* Low accuracy of tumor markers for diagnosing pancreatic neuroendocrine tumors in multiple endocrine neoplasia type 1 patients. *J Clin Endocrinol Metab.* 2013;98(10):4143-4151. <https://doi.org/10.1210/jc.2013-1800>
10. Qiu W, Christakis I, Silva A, *et al.* Utility of chromogranin A, pancreatic polypeptide, glucagon and gastrin in the diagnosis and follow-up of pancreatic neuroendocrine tumours in multiple endocrine neoplasia type 1 patients. *Clin Endocrinol (Oxf).* 2016;85(3): 400-407. <https://doi.org/10.1111/cen.13119>
11. Niederle B, Selberherr A, Bartsch DK, *et al.* Multiple endocrine neoplasia type 1 and the pancreas: diagnosis and treatment of functioning and non-functioning pancreatic and duodenal neuroendocrine neoplasia within the MEN1 syndrome – an international consensus statement. *Neuroendocrinology.* 2021;111(7):609-630. <https://doi.org/10.1159/000511791>
12. Thakker RV, Newey PJ, Walls GV, *et al.* Clinical practice guidelines for multiple endocrine neoplasia type 1 (MEN1). *J Clin Endocrinol Metab.* 2012;97(9):2990-3011. <https://doi.org/10.1210/jc.2012-1230>
13. Rockall AG, Reznick RH. Imaging of neuroendocrine tumours (CT/MR/US). *Best Pract Res Clin Endocrinol Metab.* 2007;21(1):43-68. <https://doi.org/10.1016/j.beem.2007.01.003>
14. Ito T, Jensen RT. Imaging in multiple endocrine neoplasia type 1: recent studies show enhanced sensitivities but increased controversies. *Int J Endocr Oncol.* 2016;3(1):53-66. <https://doi.org/10.2217/ije.15.29>
15. Newey PJ, Newell-Price J. MEN1 surveillance guidelines: time to (Re)Think? *J Endocr Soc.* 2022;6(2):bvac001. <https://doi.org/10.1210/jendso/bvac001>
16. Morgat C, Vélayoudom-Céphise FL, Schwartz P, *et al.* Evaluation of (68)Ga-DOTA-TOC PET/CT for the detection of duodeno-pancreatic neuroendocrine tumors in patients with MEN1. *Eur J Nucl Med Mol Imaging.* 2016;43(7):1258-1266. <https://doi.org/10.1007/s00259-016-3319-3>
17. Patil VA, Goroshi MR, Shah H, *et al.* Comparison of 68Ga-DOTA-NaI3-Octreotide/tyr3-octreotate positron emission tomography/computed tomography and contrast-enhanced computed tomography in localization of tumors in multiple endocrine neoplasia 1 syndrome. *World J Nucl Med.* 2020;19(2):99-105. https://doi.org/10.4103/wjnm.WJNM_24_19
18. Lastoria S, Marciello F, Faggiano A, *et al.* Role of (68)Ga-DOTATATE PET/CT in patients with multiple endocrine neoplasia type 1 (MEN1). *Endocrine.* 2016;52(3):488-494. <https://doi.org/10.1007/s12020-015-0702-y>
19. Albers MB, Librizzi D, Lopez CL, *et al.* Limited value of Ga-68-DOTATOC-PET-CT in routine screening of patients with multiple endocrine neoplasia type 1. *World J Surg.* 2017;41(6): 1521-1527. <https://doi.org/10.1007/s00268-017-3907-9>
20. Menntrey C, Le Bras M, Bando-Delaunay A, *et al.* Value of somatostatin receptor PET/CT in patients with MEN1 at various stages of their disease. *J Clin Endocrinol Metab.* 2022;107(5):e2056-e2064. <https://doi.org/10.1210/clinem/dgab891>
21. Froeling V, Elgeti F, Maurer MH, *et al.* Impact of Ga-68 DOTATOC PET/CT on the diagnosis and treatment of patients with multiple endocrine neoplasia. *Ann Nucl Med.* 2012;26(9): 738-743. <https://doi.org/10.1007/s12149-012-0634-z>
22. Sadowski SM, Millo C, Cottle-Delisle C, *et al.* Results of (68) Gallium-DOTATATE PET/CT scanning in patients with multiple endocrine neoplasia type 1. *J Am Coll Surg.* 2015;221(2): 509-517. <https://doi.org/10.1016/j.jamcollsurg.2015.04.005>
23. Majala S, Seppänen H, Kemppainen J, *et al.* Prediction of the aggressiveness of non-functional pancreatic neuroendocrine tumors based on the dual-tracer PET/CT. *EJNMMI Res.* 2019;9(1):116. <https://doi.org/10.1186/s13550-019-0585-7>
24. Newey PJ, Jeyabalan J, Walls GV, *et al.* Asymptomatic children with multiple endocrine neoplasia type 1 mutations may harbor nonfunctioning pancreatic neuroendocrine tumors. *J Clin Endocrinol Metab.* 2009;94(10):3640-3646. <https://doi.org/10.1210/jc.2009-0564>
25. Haneveld MJK, van Treijen MJC, Pieterman CRC, *et al.* Initiating pancreatic neuroendocrine tumor (pNET) screening in young MEN1 patients: results from the DutchMEN study group. *J Clin Endocrinol Metab.* 2021;106(12):3515-3525. <https://doi.org/10.1210/clinem/dgab569>
26. Dy BM, Que FG, Thompson GB, *et al.* Metastasectomy of neuroendocrine tumors in patients with multiple endocrine neoplasia type 1. *Am J Surg.* 2014; 208(6):1047-1053; discussion 1052-1053. <https://doi.org/10.1016/j.amjsurg.2014.08.010>
27. van Leeuwen RS, Pieterman CRC, May AM, *et al.* Health-related quality of life in patients with multiple endocrine neoplasia type 1. *Neuroendocrinology.* 2021;111(3):288-296. <https://doi.org/10.1159/000508374>
28. van Beek DJ, Pieterman CRC, Wessels FJ, *et al.* Diagnosing pancreatic neuroendocrine tumors in patients with multiple endocrine neoplasia type 1 in daily practice. *Front Endocrinol (Lausanne).* 2022;13:926491. <https://doi.org/10.3389/fendo.2022.926491>
29. Imperiale A, Meuter L, Pacak K, Taïeb D. Variants and pitfalls of PET/CT in neuroendocrine tumors. *Semin Nucl Med.* 2021;51(5): 519-528. <https://doi.org/10.1053/j.semnuclmed.2021.03.001>
30. van der Molen AJ, Schilham A, Stoop P, Prokop M, Geleijns J. A national survey on radiation dose in CT in The Netherlands. *Insights Imaging.* 2013;4(3):383-390. <https://doi.org/10.1007/s13244-013-0253-9>
31. Armstrong IS, James JM, Williams HA, Kelly MD, Matthews JC. The assessment of time-of-flight on image quality and quantification with reduced administered activity and scan times in 18F-FDG PET. *Nucl Med Commun.* 2015;36(7):728-737. <https://doi.org/10.1097/MNM.0000000000000305>
32. Cuthbertson DJ, Barriuso J, Lamarca A, *et al.* The impact of ⁶⁸Gallium DOTA PET/CT in managing patients with sporadic and familial pancreatic neuroendocrine tumours. *Front Endocrinol (Lausanne).* 2021;12:654975. <https://doi.org/10.3389/fendo.2021.654975>